Supporting Information for:
Correlations between the electronic properties of *Shewanella oneidensis* cytochrome *c* nitrite reductase (ccNiR) and its structure: effects of heme oxidation state and active site ligation

Natalia Stein, Daniel Love, Evan T. Judd, Sean J. Elliott, Brian Bennett, A. Andrew Pacheco

S1. Spectropotentiometric titration of ccNiR in the absence of cyanide

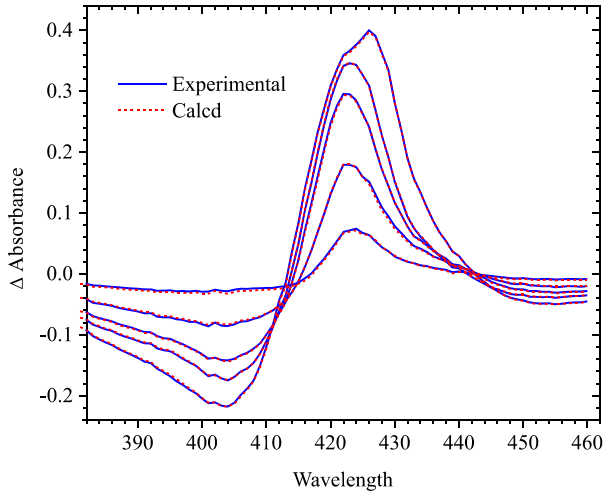

Figure S1. UV/Vis spectral changes obtained upon exposing a solution of 23.3 μM ccNiR dimer to applied potentials of –107 mV, –197 mV, –247 mV, –307 mV and –507 mV vs. SHE. Solid blue lines show the experimentally obtained data, whereas the dashed red lines were calculated from least-squares fitting to five potentials as described in ref. 10.

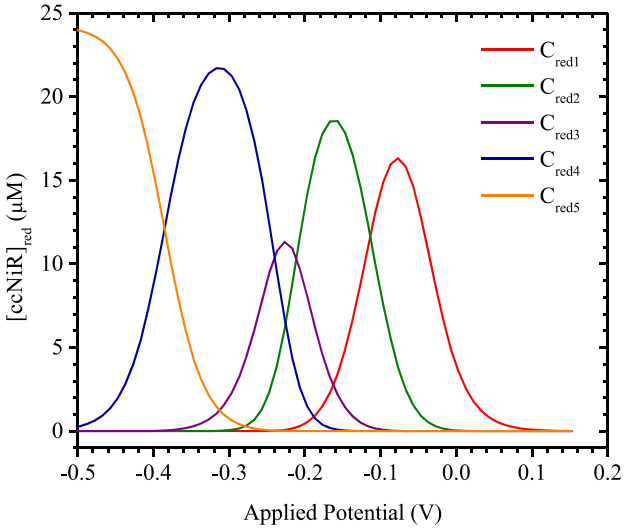

Figure S2. Concentrations of C_{red1} - C_{red5} as a function of applied potential (vs SHE) calculated for the spectropotentiometric data of Fig. S1. The corresponding extinction coefficient difference spectra are shown in Fig. 8b of the main text.

S2. Expanded EPR spectrum of ccNiR during spectropotentiometric titration

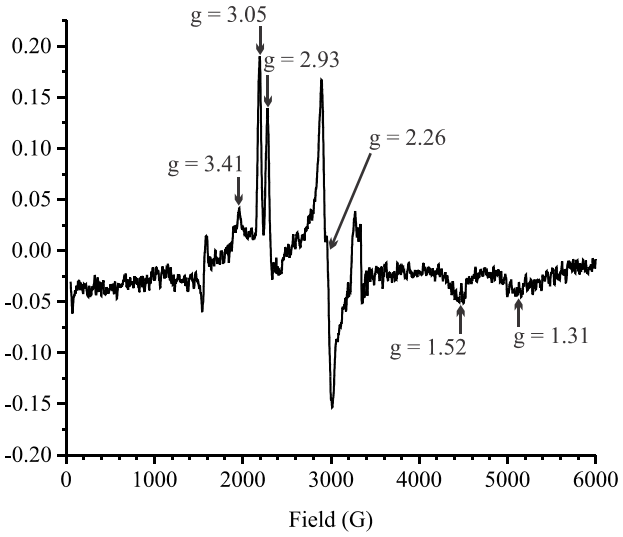

Figure S3. X-band EPR spectrum obtained for a solution initially containing 25 μM of fully oxidized ccNiR dimer in the absence of cyanide, upon exposing it to an applied potential of –235 mV vs SHE. This is one of the spectra from Fig. 6 in the main text, but expanded to show the g = 1.31 signal. This signal was seen in the presence of cyanide as well.

S3. Analysis of the UV/Vis spectropotentiometric titration of ccNiR$_{H268M}$

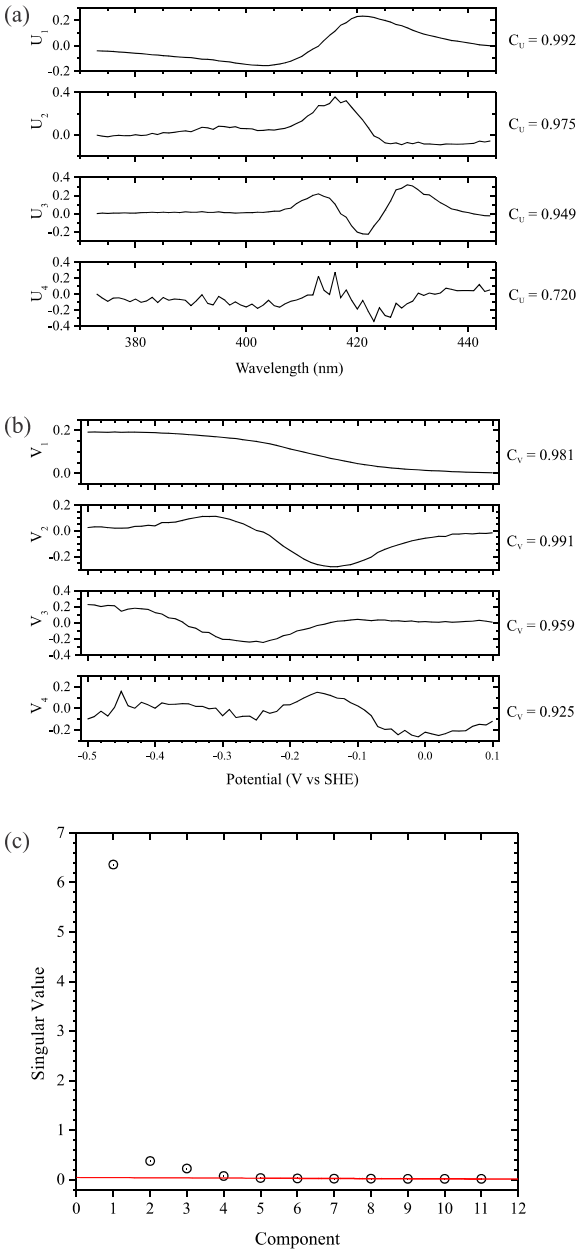

Figure S4. Results of the SVD analysis. (a) The 4 U components corresponding to singular values above the noise level, and their associated autocorrelation values C_U. (b) The 4 V components corresponding to singular values above the noise level, and their associated autocorrelation values C_V. (c) Singular values for the first 11 components.

As seen in Fig. S4, SVD analysis of the spectropotentiometric data collected for the ccNiR$_{H268M}$ mutant revealed only four spectral components above the noise, as determined by the shapes and autocorrelations of the U and V components, the relative magnitudes of the singular values *(10,26,27)*, and most importantly, by the fact that the spectra reconstructed from 4 SVD components were indistinguishable from the raw data except for being significantly less noisy. Spectra reconstructed with three or less SVD components were distorted when compared to the raw spectra. Given that ccNiR has 5 hemes in distinct environments, one would expect the spectropotentiometric titration of ccNiR$_{H268M}$ to yield 5 components, as is seen for wild type ccNiR. However, one can see from the titrations of the wild type protein (e.g. Fig. 3a) that many of the extinction coefficient difference spectra of the various partially reduced ccNiR species differ from each other only slightly. Using synthetic data to simulate SVD analysis we have often noted that, unless spectra are intense and have high signal-to-noise, very similar components will be averaged together by the SVD process. This is likely what happened during the analysis of the ccNiR$_{H268M}$ data. Due to low availability of protein, the experiments with ccNiR$_{H268M}$ were performed using less concentrated solutions, and the signal-to-noise ratios appear to have been too low to allow 5 components to be resolved.

Despite the presence of only 4 spectral components in the SVD, attempts to fit the SVD-processed data with only 4 Nernstian reduction processes yielded very poor results, suggesting that perhaps 5 Nernstian components would be detectable when looking at the non-linear applied potential dependence. The following analysis supports this conjecture.

As in previous cases *(10)* the concentration $C_{red(m)}$ of each n-electron reduced species (Scheme 1) was modeled with a Nernstian component given by Eq. S1:

$$C_{red(m)} = \frac{C_T \prod_{m=1}^{5} E_m}{denom} \qquad \text{Eq. S1a}$$

where:

$$denom = 1+E_1\{1+E_2[1+E_3[1+E_4(1+E_5)]]\}, \qquad \text{Eq. S1b}$$

$$E_m = \exp\left[\frac{nF}{RT}(\varepsilon_m^0 - \varepsilon_{app})\right] \qquad \text{Eq. S1c}$$

In Eq. S1 ε_m^0 is the midpoint potential for 1-electron reduction of the $(m-1)^{th}$ reduced species, ε_{app} is the applied potential, and C_T is the total ccNiR concentration.

For the five reduced species to give rise to only four spectrally distinct components, two out of the five would have to share extinction coefficient difference spectra that had identical shapes, though not necessarily identical intensities. For example, suppose that $C_{red(1)}$ and $C_{red(2)}$ share identically shaped extinction coefficient difference spectra. Then we could define an apparent concentration as in Eq. S2:

$$C_{red(1')} = frac \cdot C_{red(1)} + (1 - frac) \cdot C_{red(2)} \qquad \text{Eq. S2}$$

where frac is an adjustable parameter with value from 0 to 1, which allows C_{red1} and C_{red2} to have extinction coefficient spectra with different intensities. Next we could define a matrix of concentrations $\mathbf{C_{red}}$:

$$\mathbf{C_{red}} = [\overline{C_{red(1')}}, \overline{C_{red3}}, \overline{C_{red4}}, \overline{C_{red5}}] \qquad \text{Eq. S3}$$

where the vectors $\overline{C_{red(1')}} - \overline{C_{red(5)}}$ are the matrix's columns, each row of which corresponds to a unique applied potential. With $\mathbf{C_{red}}$ thus defined, the extinction coefficient difference spectrum for each apparent or true concentration could be determined using Eq. S4:

$$\mathbf{\Delta\varepsilon} = \mathbf{\Delta A} \cdot [\mathbf{C_{red}}(\mathbf{C_{red}^T C_{red}})^{-1}] \cdot \frac{1}{l} \qquad \text{Eq. S4}$$

In Eq. S4 $\mathbf{\Delta\varepsilon}$ is the matrix of extinction coefficient difference spectra in which each column coresponds to a unique reduced species, and each row corresponds to a wavelength. $\mathbf{\Delta A}$ is the SVD-processed absorbance difference matrix in which each column contains a spectrum at a fixed applied potential, and each row shows how the absorbance varies with potential at a fixed wavelength. The scalar l is the pathlength of the OTTLE cell. This equation is identical to that used in previous analyses [(10)], except that the first column of $\mathbf{C_{red}}$ is a composite of two

concentration vectors, which affects $\Delta\varepsilon$ in kind.

The SVD-processed spectropotentiometric data collected for the ccNiR$_{H268M}$ mutant were subjected to four non-linear least squares fits using a program analogous to that described in ref. 10, with the following definitions of $C_{red(m')}$:

Fit 1: $C_{red(1')} = frac \cdot C_{red1} + (1 - frac) \cdot C_{red2}$

Fit 2: $C_{red(2')} = frac \cdot C_{red2} + (1 - frac) \cdot C_{red3}$

Fit 3: $C_{red(3')} = frac \cdot C_{red3} + (1 - frac) \cdot C_{red4}$

Fit 4: $C_{red(4')} = frac \cdot C_{red4} + (1 - frac) \cdot C_{red5}$

The results are summarized in Table S1. The best fits obtained by combining $C_{red(3)}$ with $C_{red(4)}$ or $C_{red(4)}$ with $C_{red(5)}$ yielded sums of squares an order of magnitude higher than those obtained by combining $C_{red(1)}$ with $C_{red(2)}$ or $C_{red(2)}$ with $C_{red(3)}$, and were not considered further. By contrast, the best fits obtained by combining $C_{red(1)}$ with $C_{red(2)}$ were equally good as those obtained by combining $C_{red(2)}$ with $C_{red(3)}$.

Table S1. Midpoint potentials of *S. oneidensis* ccNiR$_{H268M}$ hemes (in volts vs.SHE) obtained using fitting models in which pairs of midpoint potentials are associated with spectroscopically indistinguishable reduced heme states (see text for details).

	$C_{red(1)}$ with $C_{red(2)}$	$C_{red(2)}$ with $C_{red(3)}$	$C_{red(3)}$ with $C_{red(4)}$	$C_{red(4)}$ with $C_{red(5)}$
ε_1^0	0.067	0.060	0.012	0.010
ε_2^0	–0.033	–0.035	–0.126	–0.119
ε_3^0	–0.121	–0.116	–0.194	–0.223
ε_4^0	–0.213	–0.209	–0.222	–0.357
ε_5^0	–0.340	–0.338	–0.342	–0.350
frac[a]	0.25	0.26	0.39	0.49
SS[b]	6.93×10^{-3}	6.81×10^{-3}	0.014	0.015

[a] The adjustable parameter *frac* allows two ccNiR reduced heme states that share spectroscopically indistinguishable extinction coefficient difference spectra to nevertheless contribute unequally to the spectral intensities (see text for details).
[b] SS = sum of squares.

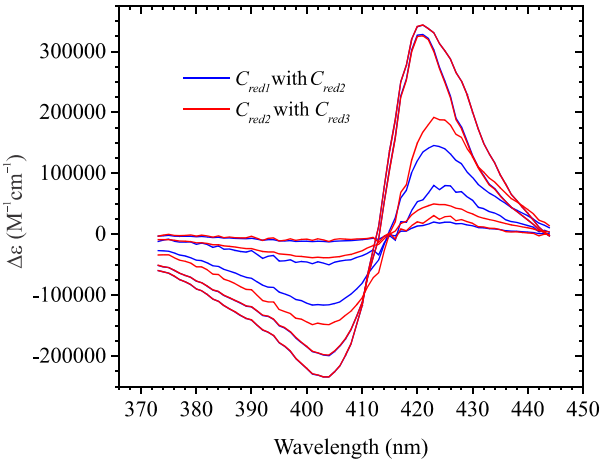

Figure S5. Extinction coefficient difference spectra corresponding to each of the reduced species $C_{red(1)}$ – $C_{red(5)}$ (Scheme 1) of $ccNiR_{H268M}$, as calculated by assuming that $C_{red(1)}$ and $C_{red(2)}$ share a commonly-shaped extinction coefficient spectrum (blue traces), or that $C_{red(2)}$ and $C_{red(3)}$ share a commonly-shaped extinction coefficient spectrum (red traces). In each case five unique extinction coefficient difference spectra are obtained by multiplying the shared difference spectrum by *frac* to split up the contributions. As expected, the magnitude of the spectral changes increases with extent of reduction.

Figure S5 compares the extinction coefficient difference spectra obtained by combining $C_{red(1)}$ with $C_{red(2)}$ with those obtained by combining $C_{red(2)}$ with $C_{red(3)}$. The only significant difference between the fitting routines is in the extinction coefficient difference spectra calculated for the 2- and 3-electron reduced $ccNiR_{H268M}$. The fitting routines give identical extinction coefficient spectra for 4- and 5-electron reduced $ccNiR_{H268M}$, and nearly identical spectra for the 1-electron reduced enzyme. Apriori, we see no compelling reason to pick one set over the other.

Figure S6a compares the extinction coefficient difference spectra obtained by combining $C_{red(1)}$ with $C_{red(2)}$ with those obtained for the wild type enzyme, while Fig. S6b does the same for the extinction coefficient difference spectra obtained by combining $C_{red(2)}$ with $C_{red(3)}$.

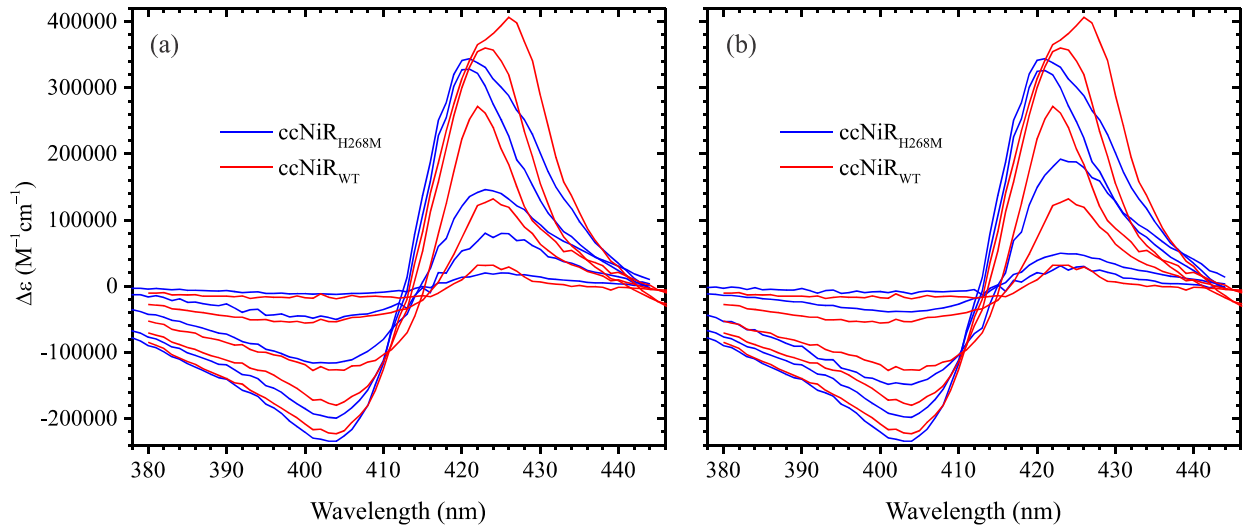

Figure S6. Comparison of the extinction coefficient difference spectra obtained for $ccNiR_{WT}$ with those obtained for $ccNiR_{H268M}$ assuming (a) that $C_{red(1)}$ and $C_{red(2)}$ share identically shaped spectra, and (b) that $C_{red(2)}$ and $C_{red(3)}$ share identically shaped spectra. Note the much-diminished red-shift in the two lowest-potential components of $ccNiR_{H268M}$, as compared to those of $ccNiR_{wt}$.